5618 *Macromolecules* **2010**, *43*, 5618–5626
DOI: 10.1021/ma1010809

Macromolecules
ARTICLE

Kinetics of Anionic Ring-Opening Polymerization of Variously Substituted β-Lactams: Homopolymerization and Copolymerization

Jihua Zhang, Samuel H. Gellman,* and Shannon S. Stahl*

Department of Chemistry, University of Wisconsin—Madison, 1101 University Avenue, Madison, Wisconsin 53706

Received May 14, 2010; Revised Manuscript Received May 24, 2010

ABSTRACT: Nylon-3 copolymers generated via ring-opening polymerization of β-lactams have recently been shown to function as selective antibacterial agents or as chemoattractants that can induce fibroblasts to attach to surfaces. Understanding the molecular basis of these activities and developing improved materials requires knowledge of the relative reactivities of different β-lactams, which influence subunit distribution patterns within polymer chains. The homopolymerization of a cyclooctyl β-lactam (**2**) in the presence of a strong base and imide co-initiator was studied using both gas chromatography (GC) and *in situ* infrared (IR) spectroscopy. The rate of this anionic ring-opening polymerization reaction exhibits a first-order dependence on the β-lactam and co-initiator concentrations and a zero-order dependence on the base concentration. Analogous studies of four other β-lactams, bearing various substituents [cyclohexyl (**1**), cyclododecyl (**3**), and Boc-protected amino groups (**4**, **5**)], revealed that different monomers exhibit significantly different homopolymerization rates. Binary copolymerizations of four β-lactam pairs (**1** + **4**, **2** + **3**, **2** + **4**, and **2** + **5**), several of which lead to biologically active amphiphilic copolymers, were investigated by GC. In each of the copolymerizations, except for **2** + **3**, the two β-lactams were consumed at different rates, leading to compositional drift within the resulting polymers (i.e., variable subunit distribution along the length of the polymer chains). The copolymerization rates of **2** + **3** and **2** + **4** exhibited a monotonic dependence on the starting β-lactam composition, whereas the copolymerization of **1** + **4** and **2** + **5** was slower than either of the respective β-lactam homopolymerizations. Three methods (Fineman−Ross, Kelen−Tudos, and Mayo−Lewis) were employed to determine the reactivity ratios of these β-lactam pairs at low conversions. This analysis confirms that the copolymers obtained from **1** + **4**, **2** + **4**, or **2** + **5** are characterized by some extent of compositional drift, while poly(**2** + **3**) is an ideally random copolymer. These results provide valuable insights pertinent to the molecular structure of amphiphilic nylon-3 copolymers that exhibit bioactivity.

Introduction

Oligomers and polymers based on β-amino acid residues are attractive for biologically oriented molecular engineering because of their similarity at the backbone level to conventional peptides and proteins derived from α-amino acids. Discrete β-peptide oligomers can mimic some conformations and functions of α-peptides.[1−3] Recently, we have begun to explore poly-β-peptides, i.e., nylon-3 polymers, which can display interesting biological properties. For example, we have identified cationic/hydrophobic nylon-3 copolymers that mimic activities of natural host-defense peptides, including selective toxicity toward bacteria relative to eukaryotic cells.[4−6] The antibacterial effects of the host-defense peptides themselves have been rationalized based on their sequences and the display of side-chain functionality that results from adoption of specific folding patterns. In contrast, the nylon-3 copolymers are polydisperse in terms of subunit sequence and stereochemistry, and their activity cannot arise from adoption of a single, specific conformation. Another effort has identified nylon-3 copolymers that can attract fibroblasts to surfaces.[7]

Our biologically active nylon-3 copolymers have been generated by anionic ring-opening polymerization (ROP) of β-lactams.[8] These reactions employ binary β-lactam mixtures with the intent to generate sequence-random copolymers. If the reactivities of the two β-lactams differ, however, then the pattern of subunits along the nylon-3 chain will not be completely random.

*Corresponding authors. E-mail: gellman@chem.wisc.edu; stahl@chem.wisc.edu.

Relatively little information is available regarding the relationship between β-lactam substitution pattern and reactivity because previous reactivity studies have been limited to β-lactams with hydrocarbon substituents.[9,10] The present study was motivated by our desire to understand how variations in β-lactam structure, including different types of hydrocarbon substituents (**1**−**3**) and substituents that bear a protected amino group (**4**, **5**), influence reactivity under ROP conditions.

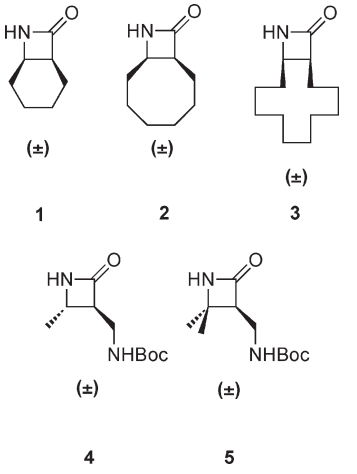

Anionic ROP of β-lactams is generally carried out with the aide of an imide co-initiator, which minimizes the length−polydispersity

 Published on Web 06/11/2010 © 2010 American Chemical Society

Scheme 1. General Mechanism of Imide-Initiated Anionic Ring-Opening Polymerization (ROP) of β-Lactams

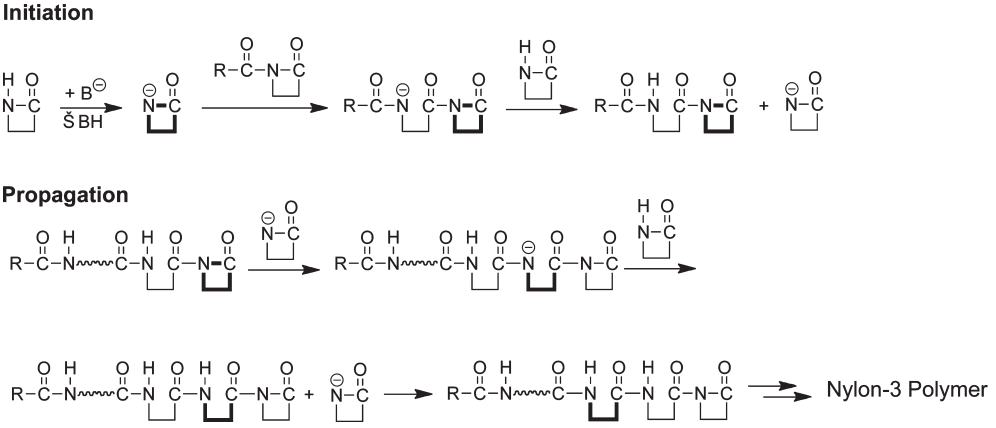

of the product polymer. Chain propagation is believed to involve nucleophilic attack of a lactamate anion on the endocyclic imide carbonyl group at the polymer chain end (Scheme 1). Recently, we have developed a modified method for anionic ROP based on the use of acylating agents such as acid chlorides or anhydrides as co-initiators for the ROP process (e.g., **I**).[11] This approach has been implemented with a variety of substituted β-lactams, including **1**−**5**, in common organic solvents. In the presence of a strong base [$LiN(SiMe_3)_2$ in the present polymerizations], the acylating agent presumably reacts rapidly with a β-lactamate, leading to *in situ* formation of an imide, which is the true co-initiating species.

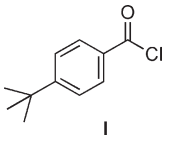

I

Several groups have investigated the kinetics of β-lactam homopolymerization;[8] however, the methods used for these studies have limitations. Some measurements are indirect, such as monitoring temperature or viscosity changes in the reaction mixture. Other approaches involve tedious product isolation prior to spectroscopic analysis. Below we report convenient methods to study ROP kinetics by directly monitoring β-lactam concentration in the reaction mixture, and we analyze the influence of polymerization kinetics for different monomers on the structure of nylon-3 copolymers. The results provide valuable insights into the molecular composition of these materials, several of which are precursors to amphiphilic polymers with important biological activities.[4−7]

Experimental Section

Materials. β-Lactams **1**−**5** were prepared according to previously reported methods.[11] $LiN(SiMe_3)_2$, 4-*tert*-butylbenzoyl chloride (**I**), benzoic acid, and THF (anhydrous, inhibitor free) were purchased from Aldrich (Milwaukee, WI) and used without further purification.

Polymerization Procedure. In a nitrogen-purged glovebox, a β-lactam, or a mixture of two β-lactams with a defined molar ratio, and triphenylmethane (internal standard) were weighed and dissolved in THF, followed by the addition of 4-*tert*-butylbenzoyl chloride co-initiator (5 mol % with respect to the total amount of β-lactam) from a premade stock solution. The mixture was allowed to stir for 5 min before being transferred to a Schlenk-type flask. A solution of $LiN(SiMe_3)_2$ in THF was prepared in a separate Schlenk-type flask. The total initial concentration of β-lactam was 0.10 mol/L unless otherwise indicated. The flasks were sealed, brought out of the glovebox, and placed into a constant-temperature heating bath. After thermal equilibration, an aliquot of solution corresponding to 12.5 mol % $LiN(SiMe_3)_2$ relative to the concentration of β-lactam was transferred using an airtight syringe into the monomer-containing flask to initiate the polymerization.

Kinetic Studies Based on Gas Chromatography (GC). GC was employed to determine β-lactam consumption. In the measurements, aliquots of polymerization solution were taken and transferred to vials containing a small amount of benzoic acid solution (quencher). The quenched reaction solutions were injected into a Shimadzu GC-17A gas chromatograph equipped with an RTX-5 column. Monomer concentration was calculated from the peak area ratio relative to a known amount of the internal standard.

Kinetic Studies Based on *in Situ* Infrared (IR) Spectroscopy. Monomer concentration was monitored in real time on a Hamilton Sundstrand Analect ChemEye FTIR analyzer using either a flow cell or an attenuated total reflection (ATR) probe, in the range 1000−2000 cm^{-1}. A sealed three-arm reaction flask containing a solution of β-lactam monomer(s) and co-initiator in THF was prepared in a nitrogen-purged glovebox, along with another sealed flask containing $LiN(SiMe_3)_2$ in THF. After the three-arm reaction flask was connected with the instrument and the solution was temperature-equilibrated, $LiN(SiMe_3)_2$ was injected using an airtight syringe to initiate polymerization. IR spectra were recorded by using the FX 90 program with a sampling interval of 6 seconds and 4 scans per sampling. IR absorbance was converted into concentration according to predetermined calibration curves.

Results and Discussion

Homopolymerization of β-Lactams 1−5. We began by focusing on β-lactam **2**, since this molecule is easily synthesized in large quantities, and the resulting polymers dissolve well in common organic solvents. Figure 1a shows the consumption of **2** as a function of time at 0 °C as monitored by GC. The monomer was fully consumed in ∼2 h. The data can be fit to a first-order decay model, suggesting that the polymerization is first order with respect to the monomer concentration, at least over most of the time course. This behavior can be seen more clearly in the semilogarithmic pseudo-first-order plot (Figure 1b), where a linear relationship is observed up to ∼85% conversion of the monomer. The apparent rate constant (k_{obs}) derived from the linear fit is 0.024 min^{-1}.

The polymerization is more rapid at higher temperature. For instance, the time required to complete the polymerization was < 10 min at 30 °C, with k_{obs} = 0.23 min^{-1}. At this temperature, as at 0 °C, deviation from first-order kinetics occurred in the latter stages of the reaction. As a control experiment, we carried out polymerization of β-lactam **2** in the absence of co-initiator **I**, i.e., initiated with only the base ($LiN(SiMe_3)_2$). This reaction was much slower (complete

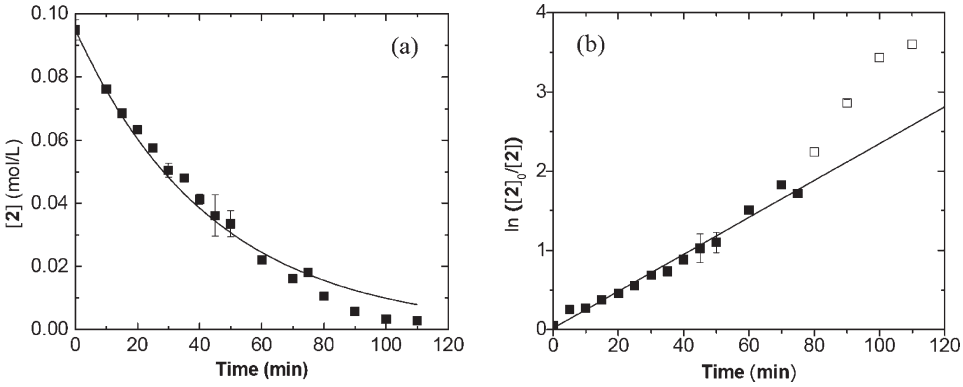

Figure 1. (a) β-Lactam starting material concentration as a function of time for the homopolymerization of **2** at 0 °C. (b) Semilogarithmic plot of the data used to generate part (a). Curves shown result from first-order exponential decay fitting for (a) and linear fitting for (b) (the last four data points (open squares) were excluded from the fit for part (b)). Conditions: [**2**] = 0.1 M, [**I**] = 0.005 M, [LiN(SiMe$_3$)$_2$] = 0.0125 M.

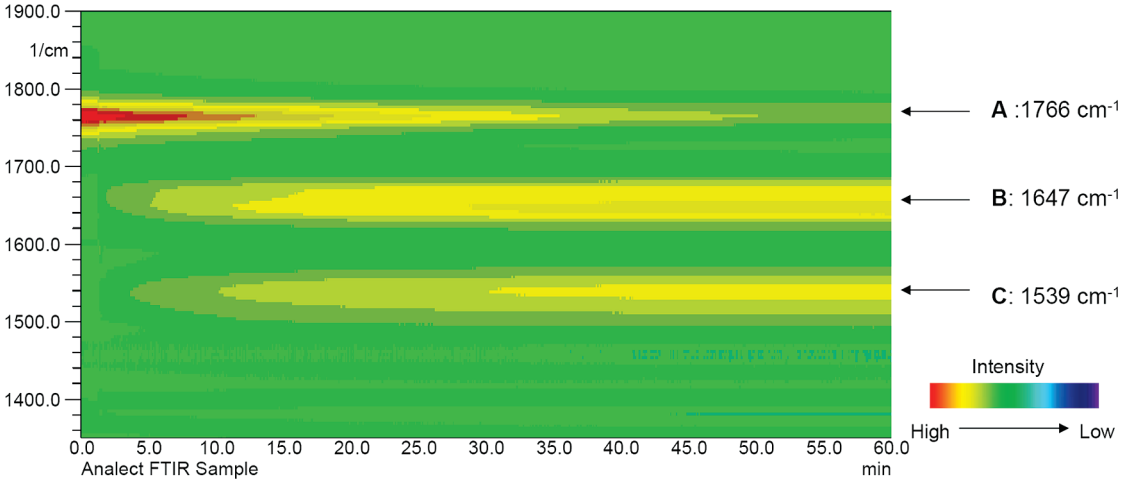

Figure 2. Temporal evolution of IR spectrum for the homopolymerization of **2** at 15 °C. Conditions: [**2**] = 0.1 M, [**I**] = 0.005 M, [LiN(SiMe$_3$)$_2$] = 0.0125 M.

consumption of **2** required 8 h at 30 °C) relative to ROP activated via inclusion of co-initiator **I**. This result indicates that the nonactivated polymerization pathway is negligible when a co-initiator is used, as in all reactions discussed below.

Deming and co-workers have observed a first-order kinetic dependence on [monomer] in the polymerization of a β-lactam derivatized from L-aspartic acid initiated by a transition metal compound Sc(N(SiMe$_3$)$_2$)$_3$.[12] Eisenbach and Lenz have previously studied anionic ROP of 3-methyl-3-alkyl-2-azetidinones,[13] one of the few types of β-lactam that has been previously found to yield polymer that is soluble in common organic solvents. These workers reported a first-order dependence of the polymerization rate on β-lactam concentration when using potassium pyrrolidone and *N*-acetylpyrrolidone as the initiator-*co*-initiator system and DMSO as the solvent, but only after ~30% conversion. Moreover, Sebenda et al. reported rather complex kinetics for anionic ROP of this type of β-lactam, and they claimed that the apparent dependence on β-lactam concentration changes during the course of polymerization.[14,15] This observation appears to be consistent with the deviation from first-order kinetics we observed toward the end of the polymerization of **2** (Figure 1).

We evaluated the dependence of the initial rate of polymerization on the concentrations of the monomer **2**, the co-initiator **I**, and the base initiator LiN(SiMe$_3$)$_2$. At monomer concentrations less than 0.1 M, the initial rate of polymerization exhibited a linear (first-order) dependence on [monomer] (Figure S1). Deviation from this dependence was observed at higher monomer concentration. On the other hand, the dependence of the initial rate of polymerization on the initial concentrations of **I** and LiN(SiMe$_3$)$_2$ was clear: the polymerization rate exhibited a first-order dependence on the co-initiator concentration [**I**] and a zero-order dependence on the concentration of the base initiator [LiN(SiMe$_3$)$_2$] (Figures S2 and S3, respectively).

We used *in situ* IR to follow anionic ROP in real time by monitoring the concentration of both the β-lactam starting material and the polymer product. β-Lactam **2** has a strong IR absorption at 1766 cm^{-1}, which arises from the C=O stretch, and the resulting polymer has two different IR signals in this region, at 1647 cm^{-1} (amide I band) and 1539 cm^{-1} (amide II band). Figure 2 shows the temporal evolution of the IR spectrum of the reaction mixture during the polymerization of **2** at 15 °C. The 1766 cm^{-1} signal (A) diminishes, which indicates depletion of monomer. Concomitantly, signals at 1647 and 1539 cm^{-1} (B and C) grow in, which indicate the formation of poly(**2**). Using external standards for calibration, we generated time courses for β-lactam consumption and polymer appearance (on a β-lactam residue basis) for the anionic ROP of **2** at this temperature (Figure 3). The decay of monomer concentration detected in this way was consistent with the GC results. The sum of the monomer and polymer concentrations stayed constant throughout the polymerization, implying that there are no side reactions and that poly(**2**) is the sole product of the reaction.

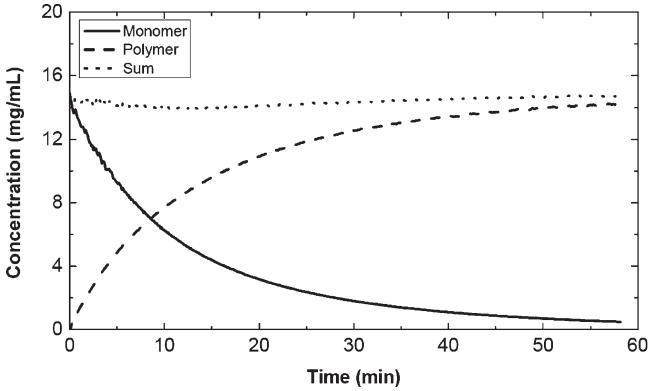

Figure 3. Time course of β-lactam consumption and polymer formation for the homopolymerization of **2** at 15 °C. The solid curve corresponds to concentration of β-lactam as determined by IR absorption at 1766 cm^{-1}, and the dashed curve corresponds to concentration of polymer, on the basis of monomer residues, as determined by IR absorption at 1647 cm^{-1}. The dotted curve is the sum of the solid and the dashed curves. Conditions: [**2**] = 0.1 M, [**I**] = 0.005 M, [LiN(SiMe$_3$)$_2$] = 0.0125 M.

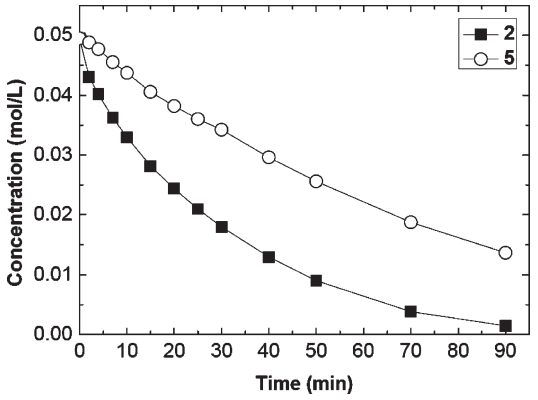

Figure 4. Dependence of the concentrations of remaining β-lactams **2** and **5** on reaction time for the copolymerization of a 1:1 molar mixture of these two starting materials. The lines simply connect the points. Conditions: [**2** + **5**] = 0.1 M, [**I**] = 0.005 M, [LiN(SiMe$_3$)$_2$] = 0.0125 M, 20 °C.

The kinetics of homopolymerization for β-lactams **1** and **3**−**5** were investigated by GC and *in situ* IR spectroscopy, and the resulting kinetic profiles of these β-lactams were similar to that of **2**. The polymerization of **1** produces a precipitate (poly(**1**) with more than 10 repeating units) within a few seconds at 20 °C, thereby precluding accurate quantitative analysis; however, a rough estimate of the rate constant for polymerization of **1** is 0.5−1 min^{-1}. The rate constant for polymerization of **3** at 20 °C is 0.033 min^{-1}, and the analogous value is 0.14 min^{-1} for **2** and 0.12 min^{-1} for **5**. β-Lactam **4** reacts so rapidly that we could not accurately measure the homopolymerization rate constant, even at 0 °C, consistent with a rate constant >1 min^{-1} at 20 °C. Comparison of the homopolymerization rate constants for β-lactams **1**−**5** establishes the following order of relative reactivity toward anionic ROP: **1** and **4** are the most reactive β-lactams; **2** and **5** are similar in reactivity and ∼5-fold more reactive than **3**. The reactivity trend among cycloalkane-derived β-lactams (**1** > **2** > **3**) and between β-lactam **4** and **5** (**4** > **5**) may arise from the increasing steric hindrance due to the presence of a larger ring (**1**−**3**) or increasing number of side-chain substituents (**4** and **5**). These trends are similar to previous observations involving other β-lactams.[16]

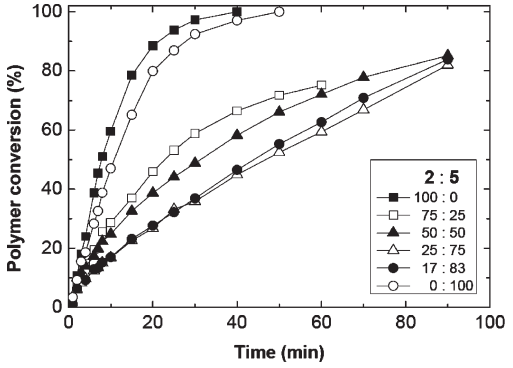

Figure 5. Extent of β-lactam conversion to polymer as a function of reaction time for copolymerization of **2** and **5** with different initial ratios. **2**:**5** = 100:0 (solid square), 75:25 (open square), 50:50 (solid triangle), 25:75 (open triangle), 17:83 (solid cycle), 0:100 (open cycle). The lines simply connect the data points. Conditions: [**2** + **5**] = 0.1 M, [**I**] = 0.005 M, [LiN(SiMe$_3$)$_2$] = 0.0125 M, 20 °C.

Binary Copolymerization of β-Lactams. We evaluated copolymerization reactions involving four β-lactam pairs: (**1** + **4**), (**2** + **3**), (**2** + **4**), and (**2** + **5**). After side-chain deprotection, three of these pairings would lead to hydrophobic/cationic nylon-3 materials of the type we have previously shown to display interesting biological activities.[4−7] For each pair, the two β-lactams were combined in various molar ratios and then subjected to conditions comparable to those used for the homopolymerization studies outlined above. We used GC to monitor the concentration of each remaining β-lactam independently during the polymerization reactions; the extent of monomer conversion and the copolymer composition were determined based on the GC data.

We begin by considering the copolymerization of **2** and **5**; the former bears a cyclooctyl unit, and the latter bears a Boc-protected amino group. Figure 4 shows the concentration of each of the β-lactams as a function of reaction time for a copolymerization started from a mixture containing a 1:1 molar ratio of **2** and **5** at 20 °C. Similar to the data described above, the initial part of each curve can be fit to a first-order function. The deduced polymerization rate constants are 0.030 min^{-1} for **2** and 0.014 min^{-1} for **5**. Each of these rate constants is substantially smaller than the corresponding homopolymerization rate constants, which are 0.13 min^{-1} for **2** and 0.12 min^{-1} for **5** at the same temperature. β-Lactam **2** is consumed more rapidly than is β-lactam **5**, which suggests that the initially formed copolymer (i.e., the N-terminal region of each final copolymer chain) contains more cyclooctyl units than protected alkylamine units. Since the polymerization continues after **2** has been completely consumed, the C-terminal region of each copolymer chain should contain more protected alkylamine units than cyclooctyl units. Thus, the kinetics suggests a somewhat uneven distribution of the two repeating units along the copolymer chain, even though a 1:1 molar ratio of monomers was employed for the polymerization reaction.

To probe the origin of this impact of copolymerization on β-lactam consumption kinetics, we examined reactions started with various **2**:**5** ratios (Figure 5). The data indicate that all of these copolymerizations are retarded compared with homopolymerization reactions. The initial rate constants (k_{obs}) for disappearance of each β-lactam were measured in these reactions. Figure 6 shows these rate constants plotted as a function of the **2**:**5** molar ratio at the start of the reaction. In each case the rate constant for β-lactam consumption is smaller than in the corresponding homopolymerization. The rate constant for consumption of β-lactam **2**

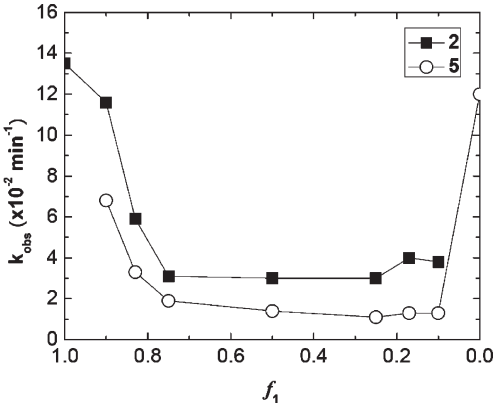

Figure 6. Plot of the apparent rate constants (k_{obs}) for consumption of **2** and **5** as a function of the fraction of **2** in the β-lactam mixture at the start of the reaction (f_1).

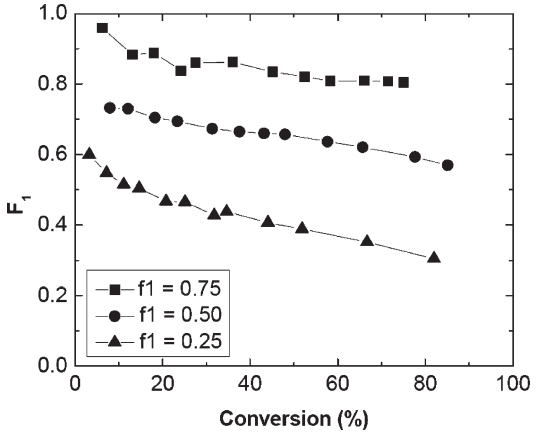

Figure 7. Subunit composition of copolymers (F_1, fraction of subunit derived from **2**) as a function of total conversion for the copolymerization of β-lactams **2** and **5**. The initial **2**:**5** proportion is indicated by f_1, which is the fraction of **2** in the starting β-lactam mixture. The lines simply connect the data points.

is larger than for consumption of **5** under all conditions, which means that all of the resulting copolymers contain a higher population of the subunit derived from **2** in their N-terminal segments than would be predicted based on the initial **2**:**5** ratio. Figure 7 shows that the copolymer composition (F_1) varies as a function of the total conversion. The impact of conversion extent on copolymer composition shows similar trends for the different initial β-lactam proportions: the polymer chains are highly enriched in subunits derived from **2** at low conversion, and the subunit proportion approaches that initial β-lactam proportion as the extent of conversion increases. Thus, if one starts with a β-lactam mixture containing 25 mol % **2**, the copolymer contains ~50 mol % subunits derived from **2** after only 10% conversion, and the copolymer contains ~40 mol % subunits derived from **2** after 50% conversion. The data in Figure 8 show how the subunit composition of a nylon-3 copolymer (F_1) depends on the initial β-lactam ratio (f_1) when the extent of conversion is limited to 10%. The diagonal (dotted line) corresponds to the composition expected at full conversion (which is equal to the initial β-lactam ratio). In all cases, as discussed above, the copolymers are enriched in subunits derived from **2**, relative to the initial β-lactam ratio. Overall, these studies show that these nylon-3 copolymers are subject to compositional drift, relative to the initial β-lactam monomer proportions, as opposed to being ideally random.

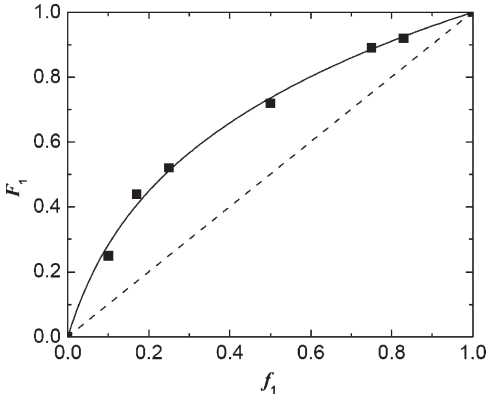

Figure 8. Composition of the copolymer (F_1 = fraction of subunits derived from **2**) as a function of the composition of the initial β-lactam mixture (f_1 = fraction of **2**) for the copolymerization of **2** and **5** at 10% conversion. The solid line shows the best fit to eq 4 (r^2 = 0.997).

To elucidate the copolymerization behavior of **2** and **5** quantitatively, we used several methods to estimate the copolymerization reactivity ratios for this system (r_1 and r_2). These ratios give a measure of the relative rates of reaction of the two different versions of living chain end (C-terminal imide derived from **2** vs C-terminal imide derived from **5**) toward each of the two different β-lactamates in the reaction mixture (β-lactamate derived from **2** vs β-lactamate derived from **5**) (Scheme 2). The rate constants k_{11} and k_{22} of the homopropagation steps (A and D), in principle, should be similar to the rate constants of the corresponding homopolymerization reactions. The rate constants k_{12} and k_{21} of the cross-propagation steps B and C) are related to k_{11} and k_{22} through the corresponding reactivity ratios, $r_1 = k_{11}/k_{12}$ and $r_2 = k_{22}/k_{21}$. For most β-lactam combinations considered here, the reactivity ratios are observed to deviate from one; in these cases, the β-lactamate species involved in the polymerization reactions preferentially react with one type of imide chain end relative to the other. It should be noted that reactivity ratios k_{11}/k_{12} and k_{22}/k_{21} for the present polymerizations do not correspond precisely to the reactions shown in Scheme 2 because the r_1 and r_2 values derived below are based on the relative reactivity of the neutral monomers. Thus, the derived r_1 and r_2 values are influenced by the relative acidities of the β-lactam monomers.[16]

We analyzed these kinetic data by two widely used linear graphical methods, Fineman−Ross[17] and Kelen−Tudos,[18−20] in order to estimate r_1 and r_2 for copolymerization of **2** and **5**. Both methods are derived from the Mayo−Lewis equation (eq 1)[21]

$$\frac{d[M_1]}{d[M_2]} = \frac{[M_1](r_1[M_1] + [M_2])}{[M_2](r_2[M_2] + [M_1])} \quad (1)$$

where M_1 and M_2 correspond to β-lactam **2** and **5**, respectively. The Fineman−Ross method is based on eq 2

$$G = r_1F - r_2 \quad (2)$$

where $F = x^2/y$ and $G = x(1 - 1/y)$; x is the instantaneous molar ratio of the two monomers in the reaction mixture, and y is the molar ratio of the subunits derived from the monomers in the copolymer at that instant. The Kelen−Tudos method is based on eq 3

$$\eta = \xi(r_1 + r_2/\alpha) - r_2/\alpha \quad (3)$$

where $\eta = G/(\alpha + F)$, $\xi = F/(\alpha + F)$, and α is defined as the positive square root of the product of the minimum and

Scheme 2. Chain Propagation Reactions of Copolymerization of 2 and 5

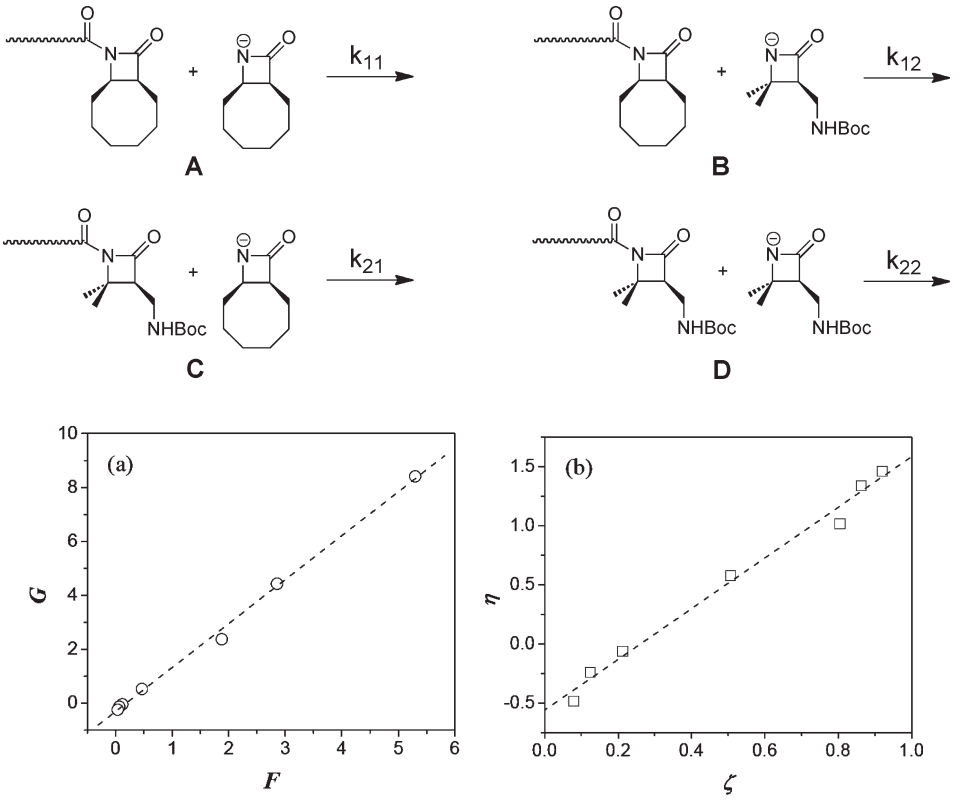

Figure 9. (a) Fineman−Ross plot and (b) Kelen−Tudos plot for the copolymerization of β-lactams **2** and **5**. See text for origin of dotted lines.

maximum value of F. The factor α helps the data points to be properly weighted. Given that both methods are most appropriate at low conversions without chain termination, we applied eqs 3 and 4 to data acquired for ≤10% conversion. The variable y was treated as the ratio of the initial reaction rates of the two monomers.

Figure 9 shows plots generated via the Fineman−Ross method (a) and the Kelen−Tudos method (b) for the copolymerization of **2** and **5**. Both plots show a good fit (correlation coefficient >0.98 in each case) to the corresponding linear equation. The reactivity ratios were determined to be $r_1 = 1.63 \pm 0.04$ and $r_2 = 0.30 \pm 0.09$ from the Fineman−Ross plot, and $r_1 = 1.58 \pm 0.10$ and $r_2 = 0.25 \pm 0.06$ from the Kelen−Tudos plot.

The subunit composition of the copolymer (F_1) can be related to the composition of the initial ratio of monomers (f_1) through the differential form of the Mayo−Lewis equation (eq 4).[22]

$$F_1 = \frac{r_1 f_1^2 + f_1(1-f_1)}{r_1 f_1^2 + 2f_1(1-f_1) + r_2(1-f_1)^2} \qquad (4)$$

Nonlinear least-squares fitting of the data in Figure 8 into eq 4 provides another way to generate the reactivity ratios for copolymerization of **2** and **5**; this approach gives $r_1 = 2.47 \pm 0.31$ and $r_2 = 0.24 \pm 0.03$ for 10% conversion. These values slightly differ from those obtained by the linear methods (Figure 9) probably because of different evaluation methods (linear vs nonlinear). It is important to note that each of the methods discussed above has limitations for determining reliable and statistically sound reactivity ratios in our case. For controlled/living polymerizations, such as anionic ROP of β-lactams, it can be problematic to determine the reactivity ratios at low conversions as the polymer chains are quite short. Nevertheless, the consistent trend in the reactivity ratios we obtained suggests that reliable qualitative conclusions can be drawn from these results.

The results summarized above ($r_1 > 1$ and $r_2 < 1$) indicate that β-lactam **2** is more reactive than β-lactam **5** toward both imide chain ends; thus, **2** is incorporated faster than **5** at early stages of the polymerization. This conclusion agrees with our observation of the progress of the copolymerization. Because r_1 and r_2 are neither very large nor very close to zero, the distribution of subunits in poly(**2** + **5**) is still expected to be approximately random. The anionic copolymerization of ε-caprolactam and ω-dodecalactam has been reported to show similar behavior, with reactivity ratios 2.26 and 0.27.[23]

We next turned our attention to a second binary copolymerization system, involving β-lactams **2** and **4**. Homopolymerization results indicated a much higher rate constant for **4** than for **2**, and we were therefore surprised to observe that copolymerization of **2** and **4** from an initial 1:1 β-lactam ratio shows similar rates of consumption for the two starting materials (Figure 10; compare with Figure 4). When the polymerization was carried out with lower initial ratios of **2**:**4**, the overall copolymerization rate increased (Figure 11), as did the rate constant for consumption of each monomer (Figure 12). This monotonic trend differs from the U-shaped trend observed for copolymerization of **2** and **5** (Figure 6). The Fineman−Ross and the Kelen−Tudos analyses (M_1 = **2** and M_2 = **4**) provided nearly identical results, with averaged reactivity ratios $r_1 = 0.75 \pm 0.04$ and $r_2 = 1.26 \pm 0.05$ (excellent linearity in both plots, Figure S5). These results reflect the higher reactivity of β-lactam **4** relative to β-lactam **2**; however, the difference is not as great as that manifested in the homopolymerization reactions. In addition, these results indicate that copolymers of **2** and **4** suffer from little compositional drift, with only slight enrichment in subunits derived

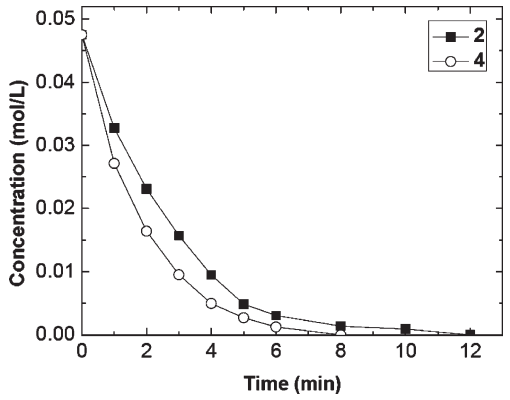

Figure 10. Dependence of the concentrations of remaining β-lactams **2** and **4** on reaction time for the copolymerization of a 1:1 molar mixture of these two starting materials. The curves simply connect the points. Conditions: [**2** + **4**] = 0.1 M, [**I**] = 0.005 M, [$LiN(SiMe_3)_2$] = 0.0125 M, 20 °C.

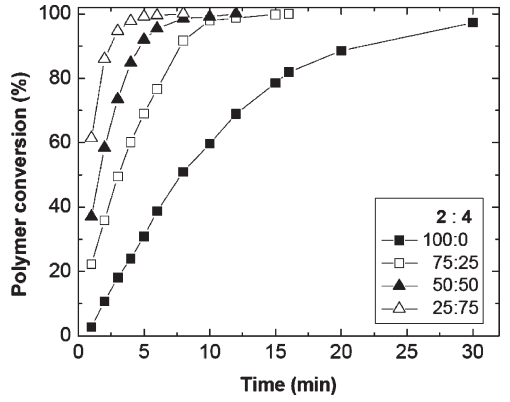

Figure 11. Extent of β-lactam conversion to polymer as a function of reaction time for copolymerization of **2** and **4** with different initial ratios. **2**:**4** = 100:0 (solid square), 75:25 (open square), 50:50 (solid triangle), 25:75 (open cycle). The curves simply connect the data points. Conditions: [**2** + **4**] = 0.1 M, [**I**] = 0.005 M, [$LiN(SiMe_3)_2$] = 0.0125 M, 20 °C.

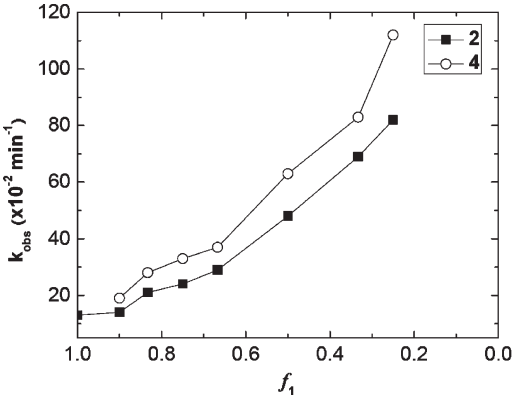

Figure 12. Plot of the apparent rate constants (k_{obs}) for consumption of **2** and **4** as a function of the fraction of **2** in the β-lactam mixture at the start of the reaction (f_1). The curves simply connect the points.

from **4** at the N-terminus and slight enrichment in subunits derived from **2** at the C-terminus. Compared to poly(**2** + **5**), poly(**2** + **4**) is closer to a random copolymer because r_1 and r_2 are closer to one.

Analogous studies were carried out for the copolymerization of **1** and **4** and for the copolymerization of **2** and **3**.

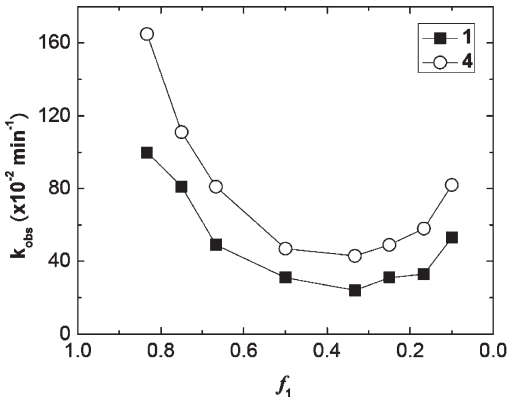

Figure 13. Plot of the apparent rate constants (k_{obs}) for consumption of **1** and **4** as a function of the fraction of **1** in the β-lactam mixture at the start of the reaction (f_1). The curves simply connect the points.

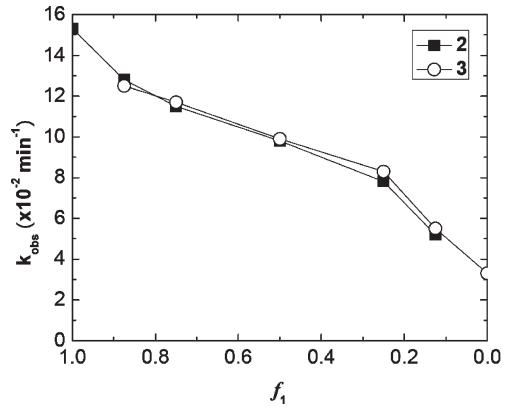

Figure 14. Plot of the apparent rate constants (k_{obs}) for consumption of **2** and **3** as a function of the fraction of **2** in the β-lactam mixture at the start of the reaction (f_1). The curves simply connect the points.

Interestingly, copolymerization data for **1** and **4** (Figure 13) exhibit the U-shaped kinetic behavior analogous to that shown for **2** and **5** in Figure 6, while the system of **2** and **3** (Figure 14) exhibits monotonic trends analogous to those seen for **2** and **4** in Figure 12. The results reveal that the β-lactam **4** is more reactive than β-lactam **1** and thus that the resulting copolymers are subject to some extent of compositional drift. In contrast, **2** and **3** are consumed at similar rates regardless of the initial β-lactam ratio, even though **2** and **3** undergo homopolymerization with a 5-fold difference in rate. Near-unity values of r_1 and r_2 derived from the copolymerization of **2** and **3** indicate that these polymers are almost ideally random. Analysis of reactivity ratios deduced for all four β-lactam pairs considered in this study (Table 1) reveals that three of the pairs feature compositional drift: poly(**1** + **4**), poly(**2** + **4**), and poly(**2** + **5**). In these three cases, one reactivity ratio is >1 and the other is <1. Since none of these reactivity ratios are very large or close to zero, all of these nylon-3 copolymers should have a fairly random distribution of subunits.

Two distinct types of copolymerization kinetics are evident among the four systems examined, with **2** + **5** and **1** + **4** displaying a suppression of overall reaction rate relative to homopolymerization, whereas **2** + **4** and **2** + **3** lack the suppression effect. One might expect the copolymerization rate to change monotonically as the fraction of one monomer varies in the starting mixture because the copolymerization should be retarded by the less active monomer. Indeed, this behavior has been found in many systems, for example,

Table 1. Summary of Reactivity Ratios for β-Lactam Copolymerizations[a]

β-lactams		Fineman−Ross[b]		Kelen−Tudos[c]		Mayo−Lewis[d]	
M_1	M_2	r_1	r_2	r_1	r_2	r_1	r_2
1[e]	**4**[e]	0.63	1.58	0.67	1.65	0.67	1.64
2	**3**	1.04	1.09	1.02	1.08	0.88	1.02
2	**4**	0.74	1.25	0.75	1.27	0.69	1.46
2	**5**	1.63	0.30	1.58	0.25	2.47	0.24

[a] Conditions: $[M_1 + M_2] = 0.1$ M, [I] = 0.005 M, $[LiN(SiMe_3)_2] = 0.0125$ M, 20 °C. [b] Values determined from the least-squares fitting of the Fineman−Ross plot. [c] Values determined from the least-squares fitting of the Kelen−Tudos plot. [d] Values determined from the best fitting of eq 4. [e] Measured at 0 °C.

radical copolymerization of styrene and acrylates.[24,25] Copolymerization reactions that proceed slower than the respective homopolymerizations, as is the case with **1** + **4** and **2** + **5**, are rather uncommon, although such situations have been theoretically predicted[26] and observed in radical copolymerization systems such as vinyl chloride−vinylidene chloride.[27] This behavior was ascribed to the large relative rate of termination between unlike radicals.[28] Such an explanation cannot apply to our systems because the anionic ROP of β-lactams has a mechanism quite different from that of radical polymerization, and chain termination is negligible in the present reactions. We can exclude physical properties of the reaction solution (e.g., viscosity) as the origin of the rate suppression seen for copolymerization of **1** + **4** or **2** + **5** because the reactions are carried out in dilute solutions (total [M] = 0.1 mol/L). It seems unlikely that the rate suppression arises from co-initiator reactivity because both 4-*tert*-butylbenzoyl chloride and a pregenerated imide co-initiator (1-benzoyl-4-phenylazetidin-2-one) give identical reaction kinetics.[11] As discussed in some previous reports on anionic ROP of β-lactams,[29,30] transacylation reactions that do not lead to chain growth (β-lactamate attack on the exocyclic carbonyl group of the C-terminal imide) may compete with chain propagation reactions (β-lactamate attack on the endocyclic carbonyl group of the C-terminal imide), and one might wonder whether the unusual copolymerization behavior we observe for **1** + **4** or **2** + **5** arises from this phenomenon. Hashimoto et al.,[31] however, have suggested that the exocyclic attack process can be neglected, since endocyclic attack is highly preferred because of β-lactam ring strain.

Our current rationale for the two distinct types of copolymerization kinetics observed here takes into account the relative pK_a values of the two β-lactams and the relative reactivities of the two imide chain ends involved in the copolymerization reactions (cf. Scheme 2). It is reasonable to expect that there will be a small difference between the acidities (pK_a) of two β-lactam monomers, and this difference in pK_a results in different ground state energies of the two β-lactamates. Proton transfer between the different β-lactamates (eq 5) is expected to be in fast equilibrium and, therefore, can be treated as a classical Curtin−Hammett

(5)

situation.[32] For reasons elaborated below, we suppose that the pK_a of β-lactams **1**−**5** decreases in the order **1** ∼ **5** > **4** > **2** > **3**. The ground state energies of corresponding β-lactamates will follow the same trend (i.e., the β-lactamate from **3** is expected to be most stable). We further assume that the differences in homopolymerization reactivity of β-lactams reflect the relative transition-state energies associated with β-lactamate attack on the corresponding imide. The fact that there is relatively little

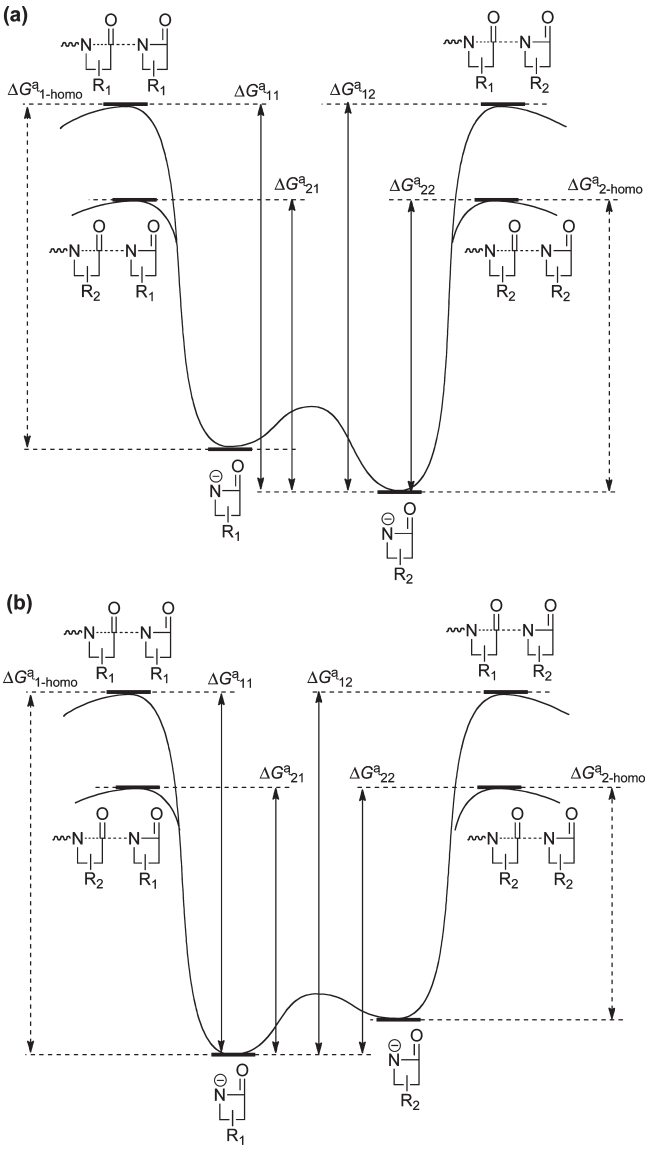

Figure 15. Schematic energy profiles for β-lactam copolymerizations. (a) Species with R_1 and R_2 side chain refer to species generated from **1** and **4**, respectively, or **5** and **2**, respectively. (b) Species with R_1 and R_2 side chain refer to species generated from **3** and **2**, respectively, or **2** and **4**, respectively.

difference in the consumption rates of β-lactams in each copolymerization suggests that the reactivity of each β-lactam is predominantly determined by the imide end group rather than the β-lactamate generated from that β-lactam. So according to our experimental results on the homopolymerization reactivity, the relative transition state energies that involve β-lactamate attack on the imide end group generated from β-lactams **1**−**5** decrease in the order **3** > **5** > **2** > **1** > **4**. These considerations provide the basis for the qualitative energy profiles for the copolymerizations shown in Figure 15.

The four β-lactam pairs in our study fit into two different types of energy profiles. β-Lactam pairs (**1** + **4**, or **2** + **5**) in which the β-lactam corresponding to the more reactive imide end group has the *lower* pK_a value are represented in Figure 15a, and β-lactam pairs (**2** + **3**, or **2** + **4**) in which the β-lactam corresponding to the more reactive imide end group has the *higher* pK_a value are described in Figure 15b. According to the Curtin−Hammett principle and the Winstein−Holness equation,[32] the overall reaction rate in a fast equilibrating system is determined by the energy difference

between the lowest-energy ground state and the respective transition states. For β-lactam pairs with the first type of copolymerization energy profile, the activation energies of the reactions involving the imide end group with R_1 side chain are higher than that of the homopolymerization of the β-lactam with R_1 side chain ($\Delta G^{\ddagger}_{11}$, $\Delta G^{\ddagger}_{12} > \Delta G^{\ddagger}_{1\text{-homo}}$). In other words, the imide end group with R_1 side chain becomes less reactive toward nucleophilic attack in the copolymerization reaction relative to that in the homopolymerization reaction. Thus, the copolymerization rate is reduced relative to the homopolymerization rate of either β-lactam. In the second copolymerization scenario, as shown in Figure 15b, the activation energies of the reactions are between those of the homopolymerization of the two β-lactams ($\Delta G^{\ddagger}_{1\text{-homo}} = \Delta G^{\ddagger}_{11} = \Delta G^{\ddagger}_{12} > \Delta G^{\ddagger}_{21} = \Delta G^{\ddagger}_{22} > \Delta G^{\ddagger}_{2\text{-homo}}$). Therefore, the overall copolymerization rate changes monotonically as the starting β-lactam ratio is varied.

Conclusion

The kinetic study of anionic ROP of β-lactams **1**−**5** co-initiated by *tert*-butylbenzoyl chloride and $LiN(SiMe_3)_2$ in THF has revealed the course of the polymerization and provided insights about the reactivity of each β-lactam. Copolymerization of four β-lactam pairs (**1** + **4**, **2** + **3**, **2** + **4**, and **2** + **5**) exhibited diverse kinetic profiles, and the variations may be attributed to combined effects of varying electrophilicities of the imide end groups derived from different β-lactams and the relative acidities of the β-lactams. Except for the pair **2** + **3**, we found that different monomers were incorporated at somewhat different rates. As a result, copolymers formed from **1** + **4**, **2** + **4**, or **2** + **5** should have some extent of compositional drift along the backbone. The copolymerization reactivity ratios (r_1 and r_2) we obtained suggest that copolymers should have random subunit arrangements, except the pair of **2** and **5**, which exhibits a slight tendency for alternating copolymerization.

The work presented here provides an important foundation for understanding the biological activities of nylon-3 copolymers generated via β-lactam ROP. The β-lactam pairs we have examined tend toward random distributions in the resulting copolymers, but in some cases there may be a preponderance of one subunit in the terminal positions. For cationic/hydrophobic pairings intended to function as selective antibacterial agents,[4−6] terminal enrichment of one type of subunit could have functional consequences. In particular, terminal enrichment of hydrophobic subunits might lead to enhanced disruptive activity toward eukaryotic cell membranes (typically detected by monitoring hemolysis), an undesirable characteristic. The optimization of nylon-3 copolymers for tissue engineering[7] and other applications will be facilitated by mechanistic insights of the type generated in the present study.

Acknowledgment. This research was supported by the NSF CRC Program (CHE-0404704) and the UW-Madison NSEC (DMR-0832760).

Supporting Information Available: Additional kinetic data (dependence of the initial polymerization rate on [**2**], [co-initiator, **I**], and $[LiN(SiMe_3)_2]$) and Fineman−Ross and Kelen−Tudos plots for the copolymerization of **1** + **4**, **2** + **4**, and **2** + **3**. This material is available free of charge via the Internet at http://pubs.acs.org.

References and Notes

(1) Gellman, S. H. *Acc. Chem. Res.* **1998**, *31*, 173–180.
(2) Cheng, R. P.; Gellman, S. H.; DeGrado, W. F. *Chem. Rev.* **2001**, *101*, 3219–3232.
(3) Seebach, D.; Hook, D. F.; Glattli, A. *Biopolymers* **2006**, *84*, 23–37.
(4) Mowery, B. P.; Lee, S. E.; Kissounko, D. A.; Epand, R. F.; Epand, R. M.; Weisblum, B.; Stahl, S. S.; Gellman, S. H. *J. Am. Chem. Soc.* **2007**, *129*, 15474–15475.
(5) Epand, R. F.; Mowery, B. P.; Lee, S. E.; Stahl, S. S.; Lehrer, R. I.; Gellman, S. H.; Epand, R. M. *J. Mol. Biol.* **2008**, *379*, 38–50.
(6) Mowery, B. P.; Lindner, A. H.; Weisblum, B.; Stahl, S. S.; Gellman, S. H. *J. Am. Chem. Soc.* **2009**, *131*, 9735–9745.
(7) Lee, M. R.; Stahl, S. S.; Gellman, S. H.; Masters, K. S. *J. Am. Chem. Soc.* **2009**, *131*, 16779–16789.
(8) Hashimoto, K. *Prog. Polym. Sci.* **2000**, *25*, 1411–1462.
(9) Graf, R.; Lohaus, G.; Boerner, K.; Schmidt, E.; Bestian, H. *Angew. Chem., Int. Ed.* **1962**, *1*, 481–488.
(10) Bestian, H. *Angew. Chem., Int. Ed.* **1968**, *7*, 278–285.
(11) Zhang, J. H.; Kissounko, D. A.; Lee, S. E.; Gellman, S. H.; Stahl, S. S. *J. Am. Chem. Soc.* **2009**, *131*, 1589–1597.
(12) Cheng, J. J.; Deming, T. J. *J. Am. Chem. Soc.* **2001**, *123*, 9457–9458.
(13) Eisenbach, C. D.; Lenz, R. W. *Macromolecules* **1976**, *9*, 227–230.
(14) Sebenda, J.; Hauer, J.; Svetlik, J. *J. Polym. Sci., Polym. Symp.* **1986**, 303–310.
(15) Sebenda, J. *Makromol. Chem., Macromol. Symp.* **1990**, *32*, 105–117.
(16) Sebenda, J. *Makromol. Chem., Macromol. Symp.* **1986**, *6*, 1–10.
(17) Fineman, M.; Ross, S. D. *J. Polym. Sci.* **1950**, *5*, 259–262.
(18) Kelen, T.; Tudos, F. *J. Macromol. Sci., Chem.* **1975**, *A 9*, 1–27.
(19) Tudos, F.; Kelen, T.; Foldesberezsnich, T.; Turcsanyi, B. *J. Macromol. Sci., Chem.* **1976**, *A 10*, 1513–1540.
(20) Kelen, T.; Tudos, F.; Turcsanyi, B. *J. Polym. Sci., Part A: Polym. Chem.* **1977**, *15*, 3047–3074.
(21) Hagiopol, C. *Copolymerization: Toward a Systematic Approach*; Kluwer/Plenum: New York, 1999.
(22) Mayo, F. R.; Lewis, F. M. *J. Am. Chem. Soc.* **1944**, *66*, 1594–1601.
(23) Frunze, T. M.; Kotelnikov, V. A.; Kurashev, V. V.; Ivanova, S. L.; Komarova, L. I.; Korshak, V. V. *J. Polym. Sci., Ser. A: Polym. Phys.* **1976**, *18*, 303–307.
(24) Fernandez-Garcia, M.; Fernandez-Sanz, M.; Madruga, E. L. *J. Polym. Sci., Part A: Polym. Chem.* **2004**, *42*, 130–136.
(25) Semsarzadeh, M. A.; Abdollahi, M. *Polymer* **2008**, *49*, 3060–3069.
(26) Melville, H. W.; Noble, B.; Watson, W. F. *J. Polym. Sci.* **1947**, *2*, 229–245.
(27) Bengough, W. I.; Norrish, R. G. W. *Proc. R. Soc. London A* **1953**, *218*, 155–163.
(28) Melville, H. W.; Valentine, L. *Proc. R. Soc. London A* **1950**, *200*, 358–375.
(29) Udipi, K.; Dave, R. S.; Kruse, R. L.; Stebbins, L. R. *Polymer* **1997**, *38*, 927–938.
(30) Budin, J.; Brozek, J.; Roda, J. *Polymer* **2006**, *47*, 140–147.
(31) Hashimoto, K.; Oi, T.; Yasuda, J.; Hotta, K.; Okada, M. *J. Polym. Sci., Part A: Polym. Chem.* **1997**, *35*, 1831–1838.
(32) Seeman, J. I. *Chem. Rev.* **1983**, *83*, 83–134.